Tin-vacancy acceptor levels in electron-irradiated n-type silicon

Larsen, A. Nylandsted; Goubet, J. J.; Mejlholm, P.; Christensen, J. Sherman; Fanciulli, M.; Gunnlaugsson, H. P.; Weyer, G.; Petersen, Jon Wulff; Resende, A.; Kaukonen, M.; Jones, R.; Öberg, S.; Briddon, P. R.; Svensson, B. G.; Lindström, J. L.; Dannefaer, S.

Published in:
Physical Review B Condensed Matter

Link to article, DOI:
10.1103/PhysRevB.62.4535

Publication date:
2000

Document Version
Publisher's PDF, also known as Version of record

Tin-vacancy acceptor levels in electron-irradiated *n*-type silicon

A. Nylandsted Larsen,* J. J. Goubet, P. Mejlholm, J. Sherman Christensen,† M. Fanciulli,‡
H. P. Gunnlaugsson, and G. Weyer
Institute of Physics and Astronomy, University of Aarhus, DK-8000 Aarhus C, Denmark

J. Wulff Petersen
The Mikroelectronic Center, The Technical University of Denmark, DK-2800 Lyngby, Denmark

A. Resende, M. Kaukonen, and R. Jones
School of Physics, University of Exeter, Exeter EX4 4QL, United Kingdom

S. Öberg
Department of Mathematics, University of Luleå, Luleå, S-971 87, Sweden

P. R. Briddon
Department of Physics, University of Newcastle upon Tyne, Newcastle upon Tyne NE1 7RU, United Kingdom

B. G. Svensson
Solid State Electronics, The Royal Institute of Technology, S-164 40 Kista-Stockholm, Sweden

J. L. Lindström
Solid State Physics, University of Lund, S-22100 Lund, Sweden

S. Dannefaer
Department of Physics, University of Winnipeg, Winnipeg, Manitoba, R3B 2E9 Canada
(Received 29 February 2000)

Si crystals (*n*-type, fz) with doping levels between 1.5×10^{14} and $2\times10^{16}\,\mathrm{cm}^{-3}$ containing in addition $\sim10^{18}\,\mathrm{Sn/cm}^3$ were irradiated with 2-MeV electrons to different doses and subsequently studied by deep level transient spectroscopy, Mössbauer spectroscopy, and positron annihilation. Two tin-vacancy (Sn-V) levels at $E_c-0.214$ eV and $E_c-0.501$ eV have been identified (E_c denotes the conduction band edge). Based on investigations of the temperature dependence of the electron-capture cross sections, the electric-field dependence of the electron emissivity, the anneal temperature, and the defect-introduction rate, it is concluded that these levels are the double and single acceptor levels, respectively, of the Sn-V pair. These conclusions are in agreement with electronic structure calculations carried out using a local spin-density functional theory, incorporating pseudopotentials to eliminate the core electrons, and applied to large H-terminated clusters. Thus, the Sn-V pair in Si has five different charge states corresponding to four levels in the band gap.

I. INTRODUCTION

Ever since the measurements by Brelot[1,2] in the beginning of the seventies of the trapping of irradiation-induced vacancies in Si by Sn impurities, Sn has been considered as one of the most efficient vacancy traps in silicon. This property has brought about the use of Sn doping of Si crystals to improve the radiation tolerance of Si-based devices.[3]

Brelot monitored, by measuring infrared (IR) absorption spectra, the concentration of di-vacancies and oxygen-vacancy pairs (*A* centers) in room-temperature (RT), electron-irradiated, Cz-grown Si containing 5×10^{18} $\mathrm{Sn/cm}^3$. No lines related to Sn could be observed. However, a reduction of the *A* center introduction rate by a factor of 13 was observed in the Sn-containing samples relative to control samples without tin. *A* centers and di-vacancies grew in as a result of annealing at about 473 K, and it was suggested that vacancies originally trapped by the Sn impurities were released at this temperature and subsequently formed the di-vacancies and *A* centers.

A similar conclusion was drawn later on by Svensson *et al.*[4] in an IR study of di-vacancies in Cz-grown silicon samples containing $\sim10^{19}\,\mathrm{Sn/cm}^3$ after high-dose electron irradiations (doses of $5\times10^{17}-2.5\times10^{18}\,\mathrm{cm}^{-2}$). Following annealing at temperatures above ~423 K a strong increase of the di-vacancy and *A*-center lines in the IR spectra was observed, and at ~463 K the di-vacancy line reached a level comparable to that of the control sample without Sn, indicating that the Sn atoms had trapped most of the produced vacancies, which were essentially all released at 463 K.

Shortly after the measurements by Brelot, Watkins[5,6] reported the results of extensive electron-spin resonance (EPR) measurements on electron irradiated, Sn containing, *p*- and *n*-type, fz Si samples. Samples doped with Sn to $\sim3\times10^{18}\,\mathrm{cm}^{-3}$ were irradiated at 20.4 K and RT. Upon annealing at ~180 K the monovacancy spectrum disappeared and a

spectrum, called Si-*G*29, grew correspondingly. Watkins concluded that the Si-*G*29 spectrum originated from the neutral charge state of a complex in which the tin atom resides at the midpoint between two unoccupied silicon-atom sites; the defect annealed at a temperature of ~500 K. This impurity-vacancy configuration is unusual as it has only been observed in the case of tin (the positive and negative charge states of the Ge-vacancy pair in Si have configurations similar to the *E*-center configuration (occupied by P-V, As-V, and Sb-V) in which both the impurity and the vacancy reside on nearest-neighbor lattice sites[7]).

Watkins and Troxell[8] concluded later, based on deep-level transient spectroscopy (DLTS) measurements of electron irradiated *p*-type Si doped with Sn, that a ~100% conversion of vacancies to these Sn-vacancy pairs takes place upon thermal annealing at ~200 K. Thus, all the vacancies produced during a low-temperature electron irradiation are trapped by the Sn atoms after a thermal annealing in *p*-type samples. In the DLTS investigation, Watkins and Troxell observed two DLTS peaks at $E_v+0.07$ and $E_v+0.32$ eV (E_v denotes the valence-band edge) which they identified as the double- and single-donor states of the Sn-vacancy defect, respectively. This behavior is quite different from that of Ge in *p*-type Si: From EPR studies, the Ge-V pair is known to assume the *E*-center configuration, as discussed above, in which the electronic structure, Jahn-Teller distortions, and level positions are very similar to those of the monovacancy in Si.[7] In agreement with this, Mesli and Nylandsted Larsen,[9] in a recent DLTS investigation of the vacancy in low-temperature electron-irradiated, strain relaxed, *p*-type SiGe alloys of low Ge content, observed only one Ge-V donor level, having the same ionization enthalpy as that of the monovacancy in pure Si. The thermal stability of the Ge-V pair, however, was found to be higher than that of the vacancy in Si.

Ion-implanted Sn in Si has been studied extensively using Mössbauer spectroscopy. Weyer *et al.*[10] reported that radioactive ^{119m}Sn implanted at RT to low doses gave rise to one unbroadened line in the Mössbauer spectrum, indicating that more than ~95% of the Sn impurities occupy undisturbed substitutional sites, and, hence, there was found no indication for a SnV-defect complex; a similar implantation of radioactive ^{119}Sb in Si[11] (^{119}Sb decays to ^{119}Sn, and the Mössbauer measurement is performed on ^{119}Sn in the configuration possibly inherited from ^{119}Sb) resulted in an additional line corresponding to a defect complex containing about 30% of the implanted Sb. Hence, from these Mössbauer measurements it was concluded that Sn is far less efficient than Sb in trapping defects.

Using *n*-type Cz-silicon samples doped with $3-6\times10^{18}$ Sn/cm^3, Svensson and Lindström[12] performed DLTS studies after low-dose irradiations by 2-MeV electrons at room temperature (doses of $1\times10^{14}-3\times10^{15}$ cm^{-2}). A substantial suppression of the generation of the V_2 and *A* centers was observed, similar to that for doses in the 10^{18} cm^{-2} range.[4] The suppression was particularly strong for the *A* center, and based on the concentrations of O_i and Sn it was estimated that Sn is about a factor of 5 more efficient than O_i as vacancy trap at room temperature.

DLTS studies of Sn related defects in electron irradiated, *n*-type, fz-silicon have been performed by Nielsen, Bonde Nielsen, and Nylandsted Larsen.[13] Tin was introduced into the Si crystal to an average density of $\sim7\times10^{19}$ cm^{-3} by ion implantation followed by rapid thermal annealing. The electron irradiations were done at a temperature slightly below RT. A Sn related deep acceptor level at $E_c-0.57$ eV was identified, which annealed at about 410 K thus somewhat lower than the anneal temperature observed by Watkins[5,6] for the SnV pair. Another DLTS line of an intensity similar to that of the Sn related line was observed at a temperature between those of the *E* center and the double-acceptor line of the di-vacancy, $VV^{=/-}$. This line was not identified by the authors.

TABLE I. Characteristics of the fz-grown, Sn doped, *n*-type, (001)-oriented Si crystals used in the present investigation. Apart from $SiSn_{III}$, which was Sb doped, all the other crystals were P doped.

Crystal	Origin	Sn Concentration (cm^{-3})	Donor Concentration (cm^{-3})
$SiSn_I$	Topsil A/S	$\sim5\times10^{17}$	1.5×10^{14}
$SiSn_{II}$	Mid-Sweden University	1.0×10^{18}	5×10^{14}
$SiSn_{III}$	Mid-Sweden University	1.5×10^{18}	2×10^{15}
$SiSn_{IV}$	Mid-Sweden University	1.0×10^{18}	2×10^{16}

In a recent EPR investigation of tin-vacancy complexes in electron irradiated *n*- and *p*-type Si samples (the *n*-type sample was from crystal $SiSn_{IV}$ described in Table I) doped with Sn to 1×10^{18} cm^{-3}, Fanciulli and Byberg[14,15] confirmed the EPR observations by Watkins for the neutral tin-vacancy complex. Moreover, they observed a defect that arose from the neutral tin-vacancy pair by a change of the charge state and they assigned this defect to the negatively charged tin-vacancy complex. Their observations indicate that the acceptor level corresponding to this change of charge state was positioned below the single-acceptor level of the divacancy ($E_c-0.42$ eV); thus, it could be the one observed by Nielsen, Bonde Nielsen, and Nylandsted Larsen at $E_c-0.57$ eV.[13] Both charge states were found to anneal at a temperature of 429 K.

Not only is the configuration of the Sn-vacancy pair in Si as observed by EPR unusual but the way Sn diffuses in silicon at high temperature has also been found to be unusual.[16] It has been established that Sn diffuses via vacancies, thus by forming Sn-vacancy complexes. However, the activation energy of diffusion is significantly higher (~0.7 eV) than expected from a comparison to Si self-diffusion via the vacancy-assisted mechanism.

The present investigation primarily focuses on the electrical properties of the Sn-vacancy pair in *n*-type Si doped with Sn as studied by DLTS after electron irradiations. It will be demonstrated that the Sn-V pair has two energy levels in the upper-half of the band gap: a single acceptor level at $E_c-0.501$ eV and a double acceptor level at $E_c-0.214$ eV, in agreement with electronic structure calculations.

II. EXPERIMENTAL PROCEDURE

A number of different Sn containing Si crystals were used in the present experiments either grown at Mid-Sweden Uni-

versity, Sundsvall or at Topsil A/S. Their principal characteristics are given in Table I. They were all *n*-type, float-zone refined crystals, doped during growth with Sn; for the crystals grown at Mid-Sweden University the tin was enriched in ^{119}Sn. The Sn concentrations were determined by secondary ion mass spectrometry (SIMS) and the donor concentrations by capacitance-voltage (CV) measurements on Schottky diodes. The $SiSn_{IV}$ crystal had a rather high carbon concentration, of the order of 10^{17} C/cm^3, whereas the other crystals contained $\sim 10^{16}$ C/cm^3 or less, as determined by IR absorption measurements. The oxygen concentrations were low in all samples ($\lesssim 1\times10^{16}$ O/cm^3).

Gold-Schottky diodes were made by deposition of *e*-gun evaporated Au through a diode-forming mask. The diodes for electron irradiations were selected according to the quality of their current-voltage (IV) and CV characteristics. No deep levels, as determined by DLTS, were observed prior to the electron irradiations.

The electron irradiations were either done at the University of Aarhus (irradiations to doses $\leqslant 10^{16}$ cm^{-2} for the DLTS measurements) or at the National Defense Research Institute, Linköping (irradiations to doses $\geqslant 10^{18}$ cm^{-2} for the Mössbauer and positron annihilation measurements). In both cases 2-MeV electrons were used and the crystals were kept at RT during irradiation. Care was taken to avoid beam heating effects. However, in the case of the high-dose irradiations, the sample temperature typically increased to 50 °C during the irradiation.

The DLTS measurements were carried out with a commercial Semitrap spectrometer using the lock-in principle to process the capacitance transient signal. Discs of about 3 mm thickness were cut from the silicon ingot (about 1 cm in diameter) and polished on both sides for Mössbauer transmission spectroscopy on the 24 keV transition of ^{119}Sn. These absorbers were mounted in a liquid-nitrogen flow cryostat for measurements at 77 and 296 K. A commercial $Ca^{119m}SnO_3$ source (15 mCi) was moved on a conventional constant acceleration drive system outside the cryostat at 296 K. The γ radiation from the source was filtered by a critical Pd absorber foil in front of the source. The γ radiation transmitted through the absorber was detected in a planar Ge detector in dependence on the relative absorber-source velocity. Positron annihilation lifetime spectra were measured on the same electron irradiated crystals as used for Mössbauer spectroscopy. Positron lifetime measurements were done at room temperature using a spectrometer with a prompt width of 210 ps at half maximum and each spectrum contained 1.2×10^7 counts. Anneals below 450 K were done in a Semitrap LN_2 cryostat in air, above 450 K in an open furnace in an N_2 ambiance.

III. RESULTS AND DISCUSSION

A. Deep-level transient spectroscopy (DLTS)

The DLTS spectra for the different samples appeared very similar and a typical example is shown in Fig. 1. Apart from lines originating from well-known and well-characterized defects[17] as indicated in the spectra, there are two dominant lines, called SnV1 and SnV2, at temperatures of 178 and 301 K, respectively. They always appeared with almost identical intensities and they were not observed in Sn-free control diodes. Thus, they are correlated to the presence of Sn and, moreover, their depth profiles, as determined by DLTS, were very similar. The apparent activation energies relative to the conduction band E_{na}, and the apparent capture cross sections σ_{na} (the so called DLTS ''finger prints'') have been extracted from Arrhenius plots of the electron emission rates e_n versus the reciprocal temperature; examples are given in Fig. 2. The electron emission rate is given by:[18]

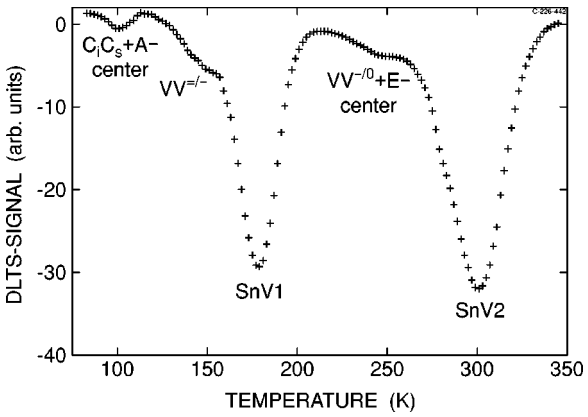

FIG. 1. DLTS spectrum of a $SiSn_{II}$ diode immediately after a 2-MeV electron irradiation at room temperature to a dose of 2.9×10^{13} e$^-$/cm^2. The spectrum was recorded with a repetition rate of 250 Hz and a filling pulse width of 140 μs.

$$e_n(T)=\chi_n N_C(T)\sigma_n(T)\langle v_n(T)\rangle\exp(-\Delta H_t/kT), \quad (1)$$

where χ_n is the entropy factor, $\chi_n=\exp(\Delta S_t/k)$, $\sigma_n(T)$ is the true capture cross section, $N_C(T)$ is the effective density-of-states in the conduction band, and $\langle v_n(T)\rangle$ is the average thermal electron velocity. The apparent activation energy contains, as will be shown shortly, a contribution E_σ from the temperature dependence of the capture cross section which, in the case of a multiphonon emission process, can be written as:[19]

$$\sigma_n(T)=\sigma_\infty\exp(-E_\sigma/kT), \quad (2)$$

where E_σ is a barrier for capture.
Thus, Eq. (1) is re-written as:

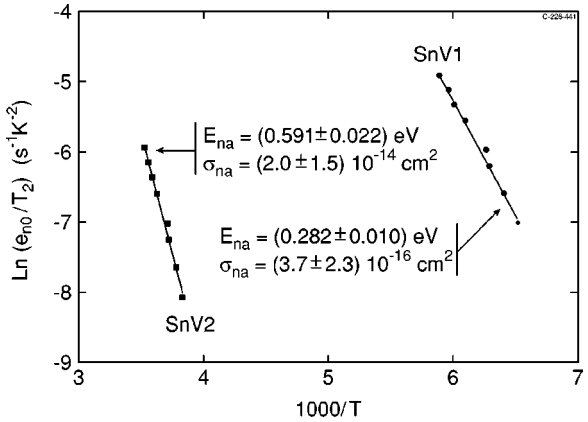

FIG. 2. Arrhenius plots of the electron emission rates for SnV1 and SnV2 of a sample from the $SiSn_I$ crystal. The DLTS ''finger prints'' for this particular sample are indicated in the figure.

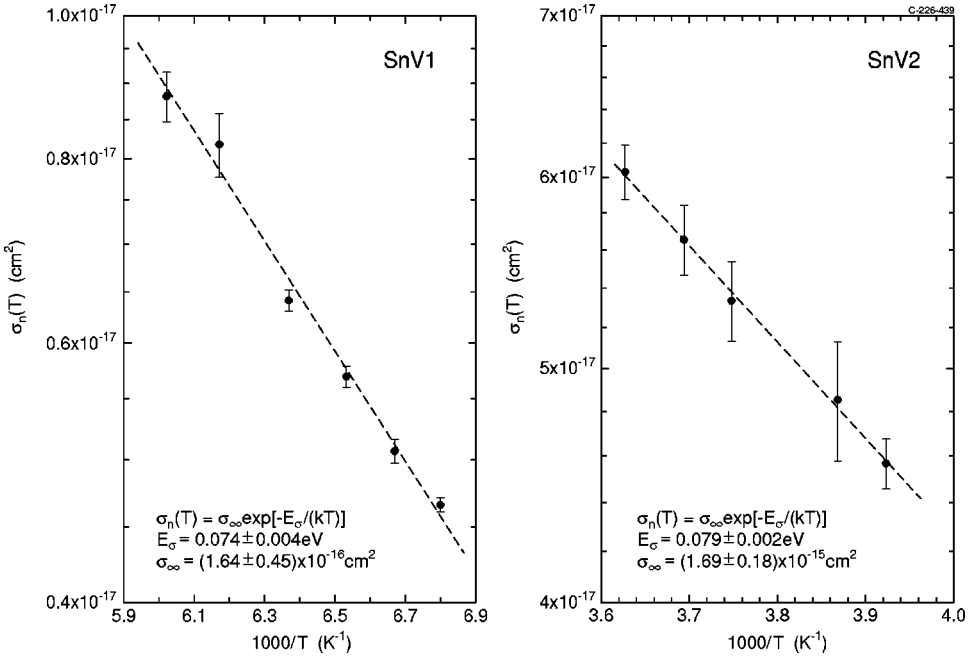

FIG. 3. Temperature dependence of the electron capture cross sections measured in a sample from the $SiSn_I$ crystal. The broken curves are exponential fits to the data points, the parameters of which are indicated in the figure.

$$e_n(T) = \chi_n N_C(T) \sigma_\infty \langle v_n(T) \rangle \exp[-(\Delta H_t + E_\sigma)/kT], \tag{3}$$

where ΔH_t is the ionization enthalpy of the trap under consideration. The apparent capture cross section is therefore

$$\sigma_{na} = \chi_n \sigma_\infty \tag{4}$$

and the apparent activation energy:

$$E_{na} = \Delta H_t + E_\sigma . \tag{5}$$

The ionization enthalpy differs from the free-energy change for ionization of the trap ΔG_t:

$$\Delta G_t(T) = \Delta H_t - T\Delta S_t , \tag{6}$$

Here, ΔS_t is the entropy change and $\Delta G_t(T)$ is equal to the separation of the energy level of the trap state from the appropriate band edge at the temperature T and is the quantity measured in, e.g., an optical excitation experiment:[18]

$$\Delta G_t(T) = E_c(T) - E_t(T). \tag{7}$$

In the present investigation the true capture cross sections were determined using the standard technique of varying the filling-pulse width.[18] This has been done as a function of temperature in order to search for any temperature dependence of the capture-cross sections. The results are presented in Fig. 3. It appears, that for both traps the temperature dependence of the capture cross sections is well represented by an exponential dependence, which is indicative of capture by multiphonon emission where E_σ is regarded as a barrier for capture.

All the parameters extracted from the DLTS analysis are collected in Table II. Please note, that the capture cross section σ_∞ is ten times larger for the SnV2 center as compared to that of the SnV1 center and that, within uncertainties, the E_σ and ΔS_t values are equal for the two centers. The observation of non-Coulombic barriers for electron capture E_σ suggests geometrical reconstructions of the defect following electron capture, i.e., the atomic configuration of the defect corresponding to trap SnV1 may not be the same as that of SnV2. The apparent activation energy of the SnV2 defect is identical to the one observed by Nielsen, Bonde Nielsen, and Nylandsted Larsen[13] for the Sn related defect in Sn implanted Si. Moreover, they also observed a peak in their DLTS spectra at almost exactly the same temperature where we observe SnV1 (the DLTS spectrum of their Fig. 1 in Ref. 13 is measured with the same repetition rate as the one used to measure the spectrum in our Fig. 1) and of the same intensity as that of their Sn-related line.

The annealing curves of the two Sn-related lines, SnV1 and SnV2, follow strictly each other in all the samples, although there are significant differences in the absolute anneal temperatures from crystal to crystal. Figure 4 shows the results of an isochronal anneal sequence on a sample from crystal $SiSn_{III}$. Prior to annealing, the intensity of SnV1 is slightly higher than that of SnV2. We consider this a result of a small hidden line below SnV1 which anneals at a tem-

TABLE II. Parameters extracted from the DLTS analysis. E_{na} and σ_{na} are average values from measurements on the four different crystals; the E_σ and σ_∞ values were only determined for sample $SiSn_I$.

Trap	E_{na} (eV)	$\sigma_{na} \times 10^{15}$ (cm^2)	$\sigma_\infty \times 10^{15}$ (cm^2)	E_σ (eV)	ΔH_t (eV)	ΔS_t
SnV1	0.288 ± 0.010	0.9 ± 0.4	0.16 ± 0.05	0.074 ± 0.004	0.214 ± 0.010	$(1.7 \pm 0.5)k$
SnV2	0.580 ± 0.011	15 ± 8	1.7 ± 0.2	0.079 ± 0.002	0.501 ± 0.011	$(2.2 \pm 0.5)k$

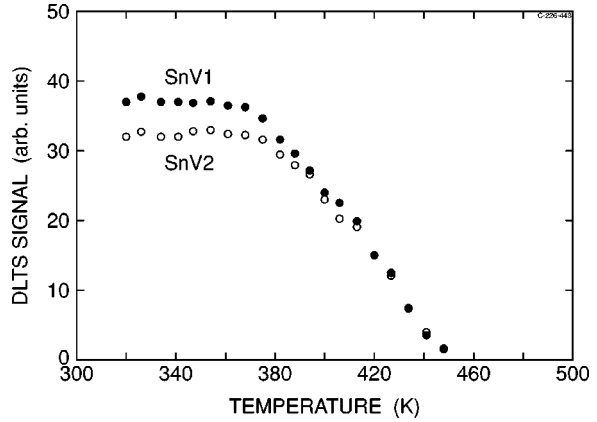

FIG. 4. Isochronal anneal sequence (30 min) of a sample from the $SiSn_{III}$ crystal irradiated with 2-MeV electrons to a dose of $3.6\times10^{14}\,e^{-}/cm^{2}$.

perature $\lesssim$390 K. In samples from the other crystals this difference was not observed. The temperature at which the as-irradiated intensity is reduced to 50% (in the following defined as the anneal temperature) has been determined to (422 ± 5) K for this particular sample. It was mentioned above that the anneal temperatures were different for the different samples. The smallest anneal temperature (380 K) was observed in samples from crystal $SiSn_{II}$ and the largest (435 K) in samples from crystal $SiSn_{I}$. We have not been able to correlate this fluctuation in anneal temperature to fluctuations in e.g., impurity concentrations or electron dose, and we have, for the time being, no explanation for this phenomenon.

A very interesting observation is the interplay between the annealing of the Sn related lines and that of the *E*- and *A* center lines. Irradiated diodes of crystal $SiSn_{IV}$, in which the *E*-center line is pronounced due to the high-phosphorus doping, were annealed at 380 K under reverse bias conditions. The *E* center is known to anneal partly under these conditions.[20] The effect of the temperature treatment was to reduce the intensity of the *E*-center line, however, the intensities of the two Sn-related lines increased correspondingly. An anneal without bias at the same temperature had no effect on the lines. Increasing the anneal temperature to 420 K without bias resulted in an increase of the *E*-center line at the expense of a similar decrease of the Sn-related lines. The system sustained several cycles, although with certain losses. The results are consistent with the following scenario: The two Sn-related lines correspond to two different charge states of the same defect, and this defect contains only one vacancy as demonstrated by the one-to-one correlation between the *E*-center and SnV intensities during the annealings. Vacancies released from the neutral charge state of the *E*-center during reverse bias annealing at 380 K are captured by Sn atoms in a one-to-one ratio. Annealing at 420 K without bias releases the vacancies from the Sn atoms to be captured by P atoms to form *E*-centers in the negative charge state (the Fermi level under these conditions is above the acceptor level of the *E* center) in a one-to-one ratio. The scenario requires quite remarkable properties of the defects involved: P must trap vacancies into the negative charge state of the *E*-center at temperatures where the neutral charge state of the *E*-center is no longer stable; Sn must trap vacancies at temperatures that are within a few degrees of its own anneal temperature. In another anneal experiment on diodes of crystal $SiSn_{IV}$, a somewhat different course was observed. The diodes were made from a part of the crystal that had been annealed at a temperature of 950 °C for 30 min in a N_2 ambiance; an annealing under such conditions in an open furnace is known to introduce a fairly high concentration of oxygen into the crystals. No *A* centers were observed after the electron irradiation, however, the annealing of SnV1 and SnV2 resulted in a corresponding increase of the *A*-center line and no increase of the *E*-center line. A similar behavior has been observed in the case of the annealing of irradiation induced GeV pairs in Si:[21] in low-oxygen containing silicon, annealing of the GeV pair resulted in a corresponding increase of the *E*-center concentration whereas in high-oxygen containing Si, the *A* center grew correspondingly.

The above results are strongly indicative of a Sn related defect containing one vacancy and with two different charge states giving rise to the two DLTS lines SnV1 and SnV2. From these experiments we cannot conclude on the number of Sn atoms involved in the defect. We know from the Mössbauer experiments, however, that prior to electron irradiation, the dominant part of the Sn atoms ($\geqslant$ 98%) is located on undisturbed substitutional sites. As Sn diffusion is not expected to take place during a room temperature electron irradiation, it is reasonable to assume that the vacancy is attached to only one Sn atom and, thus, that the center is a SnV pair.

The anneal-cycling experiments demonstrate that the SnV pair predominantly breaks up at a temperature of about 425 K rather than migrating as an entity to a trap. The same conclusion was recently reached by Fanciulli and Byberg[15] in their EPR study of Sn-vacancy complexes in high-dose $(1\times10^{18}\,e^{-}/cm^{2})$, electron irradiated Si crystals. However, they observed a conversion of the neutral SnV pair, the dominant charge state in their EPR spectra, to negatively charged V_2 and SnV_2 complexes in a two-to-one ratio, which is not observed in the present experiments. Within experimental errors no change of the intensity of the V_2 lines in the DLTS spectra upon annealing of the SnV pairs is observed. This is also in contrast to the IR results for Cz samples.[4] The much higher defect density in the samples used for the EPR and IR studies as compared to those in the samples used for the DLTS measurements is probably the major cause of this difference in anneal behavior.

The electric-field dependence of the two levels has been studied in order to indicate their acceptor or donor character; typical results are shown in Fig. 5. Whereas the electron-emission rate from the SnV2 charge state shows no dependence on the electric field, in agreement with an acceptor character,[22,23] the electron-emission rate from the SnV1 charge state has a field dependence. Its electric-field dependence is weaker than that in the case of a single donor level as demonstrated by the comparison made in Fig. 5 with the theoretical curve for the case of a single donor level, calculated according to Ref. 23.

An electric-field enhancement of the emission rate is well known and understood for a center which, after emission, remains with an opposite charge to that of the majority carrier.[22,23] This so-called Poole-Frenkel effect manifests itself as a lowering of the ionization energy induced by the

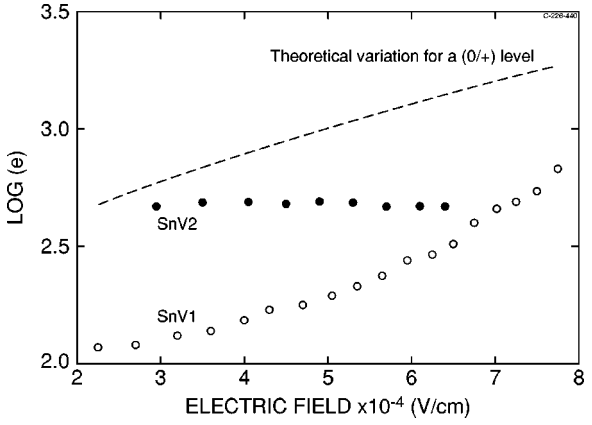

FIG. 5. The dependence of the electron emission rates on the electric field. The broken curve is a theoretical estimate of the electron-emission rate of a single donor.[23]

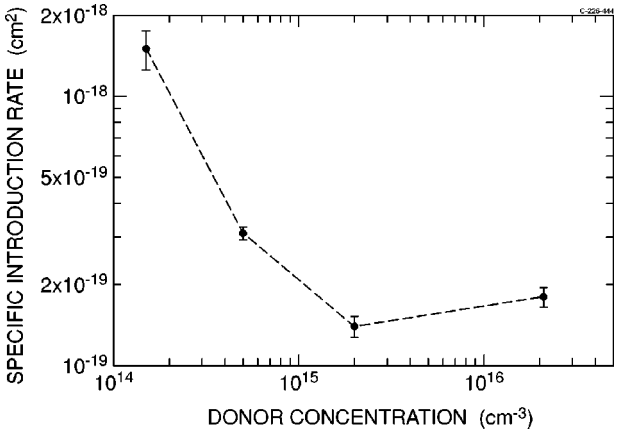

FIG. 6. The specific introduction rates as a function of donor concentration for electron doses smaller than $10^{16}\,\mathrm{cm}^{-2}$.

electric-field potential. This property is usually put forward to assign a donor or acceptor character to a deep-level defect.[24] However, this is only justified if the attractive, long-range Coulombic potential plays the dominant role in the potential shape around the defect. Indeed, as illustrated by Buchwald and Johnson in the case of the EL2 donor level in GaAs,[25] the existence of a short-range repulsive potential barrier, coincident with the one measured for thermally activated capture on the center, may reduce noticeably the field enhancement of the emission process. On the other hand, this short-range potential may also be responsible for an electric-field dependence that has been reported for electron (hole) emission from double acceptor (donor) centers, in the case, for instance, of transition-metal impurities either isolated on substitutional lattice sites[26,27] or complexed with hydrogen.[28] In this case, however, the barrier lowering for emission is much smaller than in the case of the classical Poole-Frenkel effect. The observation of a weak dependence of the emission rate of the SnV1 level on the electric-field strength is thus indicative of this center being a double acceptor.

The absence of an electric-field dependence of the emission rate of SnV2 is not sufficient to conclude that the level is a single acceptor level, as the energy barrier for electron capture is found to be 0.079 eV (see Table II). This is a large value as compared to those usually reported for other point defects in Si (0.017 eV for the double acceptor charge state of the di-vacancy, for example.[29]) This energy barrier for electron capture may thus reduce significantly any electric-field dependence induced by an attractive long-range Coulombic potential of a donor level.[25] However, as mentioned in Sec. I, recent EPR studies[14,15] indicate that the Sn-V pair has a single-acceptor level below the single-acceptor level of the di-vacancy (which is at $E_c - 0.42\,\mathrm{eV}$). Thus, we conclude that SnV2 is the single-acceptor level of the SnV pair. Both the weak electric-field enhancement of the emission rate of SnV1 and its 10 times smaller absolute capture cross section as compared to SnV2, lead us to assign the SnV1 line to the double-acceptor level of the SnV pair.

The specific introduction rates of the SnV pair have been determined for all the crystals; they are displayed in Fig. 6. As the same specific introduction rate was always found for SnV1 and SnV2, average values from the two charge states are shown in the figure. A strong influence of the background-doping concentration is observed at low-background-doping levels; at high-background-doping concentration the specific introduction rate saturates at a value of $(1.6 \pm 0.3) \times 10^{-19}\,\mathrm{cm}^2$. In the electron-dose range of the present DLTS investigations ($\leqslant 1 \times 10^{16}\,\mathrm{cm}^{-2}$) the specific introduction rate for a given donor concentration does not depend on the electron dose within the experimental errors. The specific introduction rate for the *E*-center is found to be $\sim 1.5 \times 10^{-18}\,\mathrm{cm}^2$, in good agreement with the value of $2.7 \times 10^{-18}\,\mathrm{cm}^2$ reported by Troxell[30] for a 2.4-MeV electron irradiation (the Troxell value is, however, from a sample without Sn). This demonstrates that P (and Sb) are a factor of 10 more efficient in trapping vacancies at room temperature than is Sn. For the $SiSn_{IV}$ crystal this specific introduction rate corresponds to an introduction rate of $(0.16 \pm 0.03)\,\mathrm{cm}^{-1}$, which should be compared to the introduction rate of $\sim 0.03\,\mathrm{cm}^{-1}$ reported by Fanciulli and Byberg[15] for the neutral charge state of the Watkins configuration of the Sn-V pair, $(SnV)^0$, as observed by EPR. It should be kept in mind that the electron dose used for the EPR measurements was $1 \times 10^{18}\,\mathrm{cm}^{-2}$, thus 100 times larger than the highest dose used for the DLTS measurements (an electron dose of $1 \times 10^{16}\,\mathrm{cm}^{-2}$ is close to the maximum value that can be tolerated in a DLTS experiment on diodes from sample $SnSi_{IV}$). Although the introduction rate is constant at small doses for a given donor level, as discussed above, it is anticipated to fall off at higher doses.

B. Positron annihilation spectroscopy (PAS)

In order to shed more light on the Sn-vacancy introduction rates, positron annihilation spectroscopy (PAS) measurements were performed on a 3 mm thick sample from the $SiSn_{IV}$ crystal, electron irradiated to a dose of $1 \times 10^{18}\,\mathrm{cm}^{-2}$ (this sample is similar to the samples used for the Mössbauer and EPR measurements[15]); the results were compared to results for an unirradiated $SiSn_{IV}$ sample. The vacancy concentration deduced from the PAS measurements is $(1.3 \pm 0.2) \times 10^{17}\,\mathrm{cm}^{-3}$, excluding the di-vacancy concentration. This gives an introduction rate of $(0.13 \pm 0.03)\,\mathrm{cm}^{-1}$ (the error includes an uncertainty on the electron dose of about 15%). The introduction rate, however, is an average value, as the vacancy concentration determined

from the PAS measurements was found to be nonuniform (the penetration depth of the positrons is 0.1–0.2 mm and positron irradiation of the two opposite sides of the sample gave 0.9 and 1.6×10^{17} vacancies/cm^3). The vacancy concentration deduced from the PAS measurements not only includes vacancies included in the SnV pairs but also those included in the *E* centers (and in other complexes in which the vacancy appears as a monovacancy in the PAS measurements); it can be assumed that a significant fraction of the 2×10^{16} P-atoms/cm^3 [actually $(2-5)\times10^{16}$ P-atoms/cm^3, as the P concentration in samples of the $SnSi_{IV}$ crystal varied within these limits] will be included in *E* centers, thus reducing the number of vacancies not trapped by P atoms to $(9\pm3)\times10^{16}\,\mathrm{cm}^{-3}$. This converts into an upper limit of the SnV introduction rate deduced from the PAS measurements of $(0.09\pm0.03)\,\mathrm{cm}^{-1}$ (it is an upper limit because it is assumed that the vacancies are only trapped in SnV pairs and *E* centers). This value is smaller than the one measured at low doses by DLTS, thus indicating a reduced introduction rate with increasing dose, in accordance with the one deduced from the EPR measurements.[15] The small introduction rate at very high-electron dose is also in agreement with the Mössbauer measurements as demonstrated in the following section.

C. Mössbauer spectroscopy

Measurements before the electron irradiations of the sample showed a single-line spectrum with parameters characteristic of substitutional Sn in silicon.[31] No indication of any Sn clustering or precipitation of α- or β-Sn phases was found. The spectra of such precipitates are well known as they have been detected previously upon thermal annealing of epitaxially grown $Si_{1-x}Sn_x$ layers on silicon with Sn concentrations above the solid solubility limit.[32] Following the electron irradiation, four Mössbauer spectra were measured alternately at 77 and 296 K. Debye temperatures θ were deduced from these measurements. The analysis of the spectra did not indicate any new line apart from the line for substitutional Sn [$\delta=(1.77\pm0.03)$ mm/s at 296 K and $\theta=(233\pm6)$ K]. As for such conditions Sn-vacancy complexes have been found in the same or similar samples in the EPR measurements,[14,15] the questions arise whether the Mössbauer line(s) for such complexes is/are distinguished from that of substitutional Sn and if so, whether the sensitivity of Mössbauer spectroscopy would be sufficient to detect them for the given statistical accuracy. Sn-vacancy complexes have been observed by Mössbauer spectroscopy previously, however, with (ion implanted) radioactive probe atoms and under conditions different from those of the present electron irradiations.

In the following we briefly summarize the evidence for the identification of a line with an isomer shift of $\delta_{\text{Sn-V}}=(2.3-2.4)$ mm/s, a Debye temperature of $\theta\approx170$ K, and presumably a small quadrupole splitting of $\Delta\approx0.3$ mm/s as due to SnV complexes. The line has been observed after room temperature implantations of radioactive ^{119}Cd, ^{119}In, and ^{119}Sb into silicon, which in their decay all populate the 24 keV Mössbauer state of ^{119}Sn.[33–35] Fractions of 10–30% of the probe atoms were found corresponding to this configuration, which is proposed to be formed in the radiation damage cascades by the interactions of the probe atoms with the vacancies in a locally high concentration. Remarkably, this line is not found in similar fractions upon implantations of radioactive ^{119}Sn,[31] only upon thermal treatment.[36] Furthermore, an indication of the presence of the line upon α irradiation of preannealed samples, containing substitutional ^{119}Sn, was found albeit in much lower fractions than for similar samples containing ^{119}Sb probe atoms.[35,37] With Sb probe atoms the defect was found to be completely annealed after thermal annealing at 520 K. Also for low dose ^{119}In implantations ($\leqslant10^{12}$/cm^2) complete annealing was observed at $\leqslant600$ K,[33] whereas it transformed into a line, $\delta=2.6$ mm/s, assigned to SbV complexes for high dose ^{119}Sb implantations ($\geqslant10^{13}$/cm^2) at about 400 K.[35] The annealing behavior of the SbV and InV complexes as observed by other techniques[38,39] is consistent with these results. The line assigned to SnV complexes has also been observed to be formed with both ^{119}Sb and ^{119m}Sn probe atoms in thermal equilibrium in heavily doped n^+-type material at >900 K.[40] Again larger vacancy complex fractions were formed with ^{119}Sb than with ^{119m}Sn. Thus, under all conditions discussed above, the formation probability for vacancy complexes is larger with Sb than with Sn probe atoms.

Irrespective whether the complexes are formed with different parent isotopes, however, the Mössbauer parameters of the SnV daughter complexes are the same. This suggests that the defect structure is characteristic for the Sn daughter complex and is, therefore, most likely the Watkins configuration of the SnV complex.

Given that the Mössbauer parameters for the SnV complex are known, spectra with different complex and substitutional fractions have been simulated to find a threshold fraction, which would be detectable with the present statistical accuracy. The analysis shows that fractions of 1.5% would be detectable within a 1σ confidence interval and 3% within a 3σ interval. This then gives an upper limit for the concentration of SnV complexes in the samples of a few percent. This is consistent with the introduction rate as deduced from the EPR experiment for similar doses.[14,15] The PAS results, on the other hand, imply a slightly higher fraction for the same samples as employed in the Mössbauer experiments. As such fractions should be observable in the Mössbauer spectra it is tempting to assume that vacancy complexes other than SnV and *E* centers might exist in the samples.

D. Theory

The electronic-structure calculations described here have been carried out using a local spin-density functional theory, incorporating pseudopotentials to eliminate the core electrons, and applied to large H-terminated clusters. To investigate the SnV defect, two atoms closest to the center of a 246-atom cluster were removed to create a lattice di-vacancy and, either a Sn atom was placed at its center yielding a defect with D_{3d} symmetry, or placed near to one of the vacant lattice sites giving a defect with C_{3v} symmetry. To check the influence of cluster size, some calculations were also carried out on larger clusters containing 298 atoms.

The wave functions were expanded in a basis consisting of *N* Cartesian *s*, *p* Gaussian orbitals sited on each atom. The charge density was fitted to *M* Gaussian functions. In this

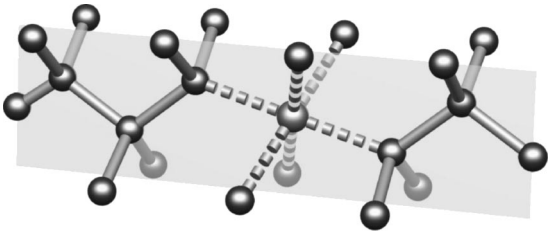

FIG. 7. Lowest-energy structure of the neutral tin split-vacancy with D_{3d} symmetry and spin-triplet ($^3A_{2g}$) ground state (Si-G29). The plane shown defines the (110) crystal directions. The tin impurity atom is six-fold coordinated with the Sn-Si bonds being 2.89 Å long.

paper, (N, M) were: (6, 6) for Sn, (4, 5) for Si, and (2,3) for H. Two extra Gaussian orbitals with different exponents, located midway between each bonded pair of atoms (excluding the H terminators), were added to the wave function basis, and similar bond-centered functions were added to the basis for the charge density. The forces on the atoms were found analytically and all atoms in the cluster were then moved, using a conjugate gradient algorithm, until the forces vanished. A detailed account of the technique can be found elsewhere.[41] The method yields the structure, energetics, ionization energies, and the electron affinities of the defect. However, to determine the electrical levels of the defect, the ionization energies and the electron affinities are compared with those of standard defects in a way described previously.[42] The accuracy of these levels is of order ± 0.2 eV.

The neutral spin-one $(\mathrm{SnV})^0$ defect, with D_{3d} symmetry, is stable and possesses six Sn-Si bonds of length 2.88 Å (Fig. 7). The $S=1$ defect is 0.174 eV lower in energy than the spin-zero defect with the same symmetry, and 0.14 eV lower in energy than a C_{3v} form ($S=1$). The spin-zero defect with C_{3v} symmetry, where Sn is located near one of the vacant lattice sites, is metastable and has 0.045 eV higher energy than the D_{3d} structure with spin 1. Thus the calculations support the structure for the defect determined from EPR.[5]

The Kohn-Sham levels of the spin-one $(\mathrm{SnV})^0$ consist of a fully $e_g^{\uparrow}$ occupied level, lying in the lower part of the gap, and above an $e_u^{\uparrow}$ level, which has merged with the valence band. There is an empty singlet lying close to the conduction band above the e_g manifold. The $e_g^{\downarrow}$ level is empty. The e manifold is then capable of losing or gaining two electrons. The wave functions for the e_g orbitals posses a node at the Sn atom (Fig. 8). This implies that the spin density at the Sn nucleus is small, consistent with EPR studies.[5]

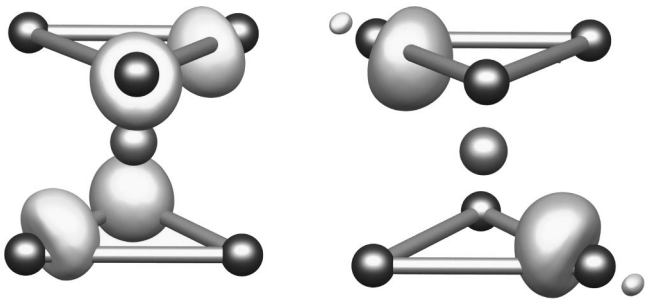

FIG. 8. 3D-isosurface wave function plot of the two highest occupied spin-up Kohn-Sham levels of $S=1$ (D_{3d}) SnV^0.

The Kohn-Sham levels give only an approximate account of the electrical activity of the defect. To determine the electrical levels as measured in a DLTS experiment, it is necessary to evaluate energy differences between states. This can be done by finding the ionization energies and electron affinities of the defect embedded in a cluster. These are total-energy differences and hence related to the donor and acceptor levels. However, the ionization energies and electron affinities are affected by the surface of the cluster but first-order perturbation theory shows that the shift caused by the surface will be the same for different defects with similar energy levels. Thus, the electronic levels of the defect were found by comparing the ionization energies and electron affinities with standard defects embedded in the same sized clusters.[42] The calculated levels are then given by those of the standard shifted by the difference in ionization energies and electron affinities. This method takes into account the effect of the cluster surface on the energy level and is more reliable if the standard defect has a level close to that of SnV. The standard defects were chosen to be substitutional Pt, the carbon interstitial C_i, and the AuH_1 and PtH_2 defects. The $(+/++)$ level of Pt lies at $E_v+0.07$ eV,[43] while C_i has $(0/+)$ and $(-/0)$ levels at $E_v+0.27$ and $E_c-0.10$ eV, respectively.[44] The $(=/-)$ levels of AuH_1 and PtH_2 at $E_c-0.19$ eV (Refs. 45 and 46) and $E_c-0.18$ eV (Ref. 47), respectively.

The calculations showed that upon relaxation $(\mathrm{SnV})^-$ remains close to D_{3d} symmetry although we cannot exclude a small Jahn-Teller distortion in agreement with the structure found experimentally by EPR (Ref. 14). The first and second ionization energies were found by starting with the D_{3d} structure and removing 1/2 e and 3/2 e, respectively, from the $e_g^{\uparrow}$ levels. The defect was then re-relaxed. According to the transition state method,[48] the ionization energy of the defect is then simply $-E(e_g^{\uparrow})$ where the energy of the partially occupied $e_g^{\uparrow}$ level is $E(e_g^{\uparrow})$. These calculations were repeated for the C_i defect and the substitutional Pt defect. The donor levels could then be found by comparing the ionization energies of these defects. The calculated $(+/++)$ and $(0/+)$ levels are $E_v+0.09$ eV and $E_v+0.22$ eV, respectively. These are in excellent agreement with the experimental values of $E_v+0.07$ eV and $E_v+0.32$ eV, respectively.[8]

In a similar way, the first and second acceptor levels were found using the electron affinity. In this case 1/2 e or 3/2 e are added to the $e_g^{\downarrow}$ level and the cluster re-relaxed. The electron affinity is then $-E(e_g^{\downarrow})$ and is compared with that of a standard defect. The $(-/0)$ level is found to lie at $E_c-0.56$ eV, again in excellent agreement with the SnV2 deep level at $E_c-0.50$ eV. The $(=/-)$ level is, however, sensitive to the marker. The use of the AuH_1 defect places the $(=/-)$ level of SnV at $E_c-0.39$ eV in reasonable agreement with SnV1 at $E_c-0.21$ eV. However, the electron affinity of $(\mathrm{SnV})^-$ is 0.4 eV greater than that of the PtH_2 defect. Originally, the $(=/-)$ level of PtH_2 was placed around $E_c-0.075$ eV (Ref. 49) giving the $(=/-)$ level of SnV at $E_c-0.475$ eV. However, further work and DLTS studies[47] have lowered the level of PtH_2 to about $E_c-0.18$ eV leading to an estimate of the $(=/-)$ level of SnV at $E_c-0.58$ eV. This sensitivity to the marker probably reflects the fact that the

wave function of either SnV or the markers, are more delocalized and significantly overlap the surface of the cluster. Nevertheless, the calculations show that SnV possesses two acceptor levels in addition to two donor ones. No further levels can arise as the e_g manifold is filled for $(SnV)^{2-}$ and empty for $(SnV)^{2+}$.

In order to study the efficiency of a tin atom as a vacancy trap, we calculated the binding energy of Sn with the neutral vacancy. The energy difference between the SnV $D_{3d}(S=1)$ defect and the neutral vacancy with a substitutional Sn atom at a second neighbor site is -0.3 eV, and -0.9 eV when the vacancy is completely separated from Sn. Thus, there is a large binding energy between Sn and vacancies.

IV. CONCLUSION

Using DLTS on electron-irradiated, Sn-containing, *n*-type Si Schottky diodes it is demonstrated that the SnV pair has two acceptor levels in the upper-half of the band gap: a $(-/0)$-level at 0.50 eV and a $(=/-)$ level at 0.21 eV, both relative to the conduction-band edge. The anneal temperature of $\sim$425 K for the SnV complex is in perfect agreement with that observed by recent EPR measurements. The introduction rate of the SnV pair determined by DLTS is significantly higher than that deduced from Mössbauer spectroscopy and positron annihilation spectroscopy. It is argued, however, that this difference is most probably due to the much larger electron dose used for these measurements. It is concluded that the two acceptor levels are charge-state levels of the SnV pair. The SnV pair, therefore, has five charge states corresponding to four levels in the band gap.

This conclusion is in agreement with electronic structure calculations which demonstrate that Sn-V has five charge states. This multitude of states is exceptional and arises from the nature of the e_g orbital which, although of bonding character, is nodal at the Sn atom. Thus the extra carriers introduced into the e_g orbital by trapping are distributed outside the core of the defect thereby reducing the electron-electron interaction.

Annealing of the SnV pairs results in a one-to-one increase of either the *A* center in samples containing a high-oxygen concentration or the *E* center in samples containing a high-phosphorus concentration but in both cases only in a minor increase of the di-vacancy signal. This is opposed to observations made in IR and EPR studies of high-electron dose irradiated crystals where substantial increases in the di-vacancy concentration follow upon annealing of the SnV pair. This effect is suggested to be due to the much higher defect density in the high-dose irradiated samples.

ACKNOWLEDGMENTS

This work was supported by the Danish Natural Scientific Research Council, and the EEC-TMR European Network on Defect Engineering of Advanced Semiconductor Devices (ENDEASD) (Contract No. ERBFMRXCT980208). Thanks are due to Pia Bomholt for preparation of the diodes.

*Corresponding author; e-mail address: anl@ifa.au.dk

†Present address: KTH, Solid State Electronics, Dept. of Electronics, Electrum 229, S-164 40 Kista, Sweden.

‡Present address: Laboratorio MDM-INFM, Via C. Olivetti 2, I-20041 Agrate Brianza (MI); Italy.

[1] A. Brelot, IEEE Trans. Nucl. Sci. **19**, 220 (1992).

[2] A. Brelot, in *Radiation Damage and Defects in Semiconductors*, edited by J. E. Whitehouse (Institute of Physics, London and Bristol, 1973), Conference Series No. 16, p. 191.

[3] Yu. M. Dobrovinskii, M. G. Sosnin, V. M. Tsmots', V. I. Shakhovtsov, and V. L. Shindich, Fiz. Tekh. Poluprovodn **22**, 1149 (1989) [Sov. Phys. Semicond. **22**, 727 (1989)].

[4] B. G. Svensson, J. Svensson, J. L. Lindström, G. Davies, and J. W. Corbett, Appl. Phys. Lett. **51**, 2257 (1987).

[5] G. D. Watkins, Phys. Rev. B **12**, 4383 (1975).

[6] G. D. Watkins, Solid State Commun. **17**, 1205 (1975).

[7] G. D. Watkins, in *Deep Centers in Semiconductors. A State-of-the-Art Approach*, edited by S. T. Pantelides (Gordon and Breach Science, New York, 1986), p. 147.

[8] G. D. Watkins and J. R. Troxell, Phys. Rev. Lett. **44**, 593 (1980).

[9] A. Mesli and A. Nylandsted Larsen, Phys. Rev. Lett. **83**, 148 (1999).

[10] G. Weyer, A. Nylandsted Larsen, B. I. Deutch, J. U. Andersen, and E. Antoncik, Hyperfine Interact. **1**, 93 (1975).

[11] G. Weyer, A. Nylandsted Larsen, N. E. Holm, and H. L. Nielsen, Phys. Rev. B **21**, 4939 (1980).

[12] B. G. Svensson and J. L. Lindström, J. Appl. Phys. **72**, 5616 (1992).

[13] J. Nielsen, K. Bonde Nielsen, and A. Nylandsted Larsen, Mater. Sci. Forum **38–41**, 439 (1989).

[14] M. Fanciulli and J. R. Byberg, Physica B **273–274**, 524 (1999).

[15] M. Fanciulli and J. R. Byberg, Phys. Rev. B **61**, 2657 (2000).

[16] P. Kringhøj and A. Nylandsted Larsen, Phys. Rev. B **56**, 6396 (1997).

[17] G. D. Watkins, in *Defects and Diffusion in Silicon Processing*, edited by T. Diaz de la Rubia, S. Coffa, P. A. Stolk, C. S. Ref MRS symposia Proceedings No. 469 (Materials Research Society, Pittisburgh, 1997).

[18] See, e.g., P. Blood and J. W. Orton, *The Electrical Characterization of Semiconductors*: *Majority Carriers and Electron States* (Academic, London, 1992).

[19] J. Bourgoin and M. Lannoo, *Point Defects in Semiconductors II*; *Experimental Aspects* (Springer-Verlag, Berlin, 1983), p. 193.

[20] L. C. Kimerling, H. M. DeAngelis, and J. W. Diebold, Solid State Commun. **16**, 171 (1975).

[21] C. V. Budtz-Jørgensen, P. Kringhøj, A. Nylandsted Larsen, and N. V. Abrosimov, Phys. Rev. B **58**, 1110 (1998).

[22] J. Frenkel, Phys. Rev. **54**, 647 (1938).

[23] J. L. Hartke, J. Appl. Phys. **39**, 4871 (1968).

[24] See for example L. C. Kimerling and J. L. Benton, Appl. Phys. Lett. **39**, 410 (1981).

[25] W. R. Buchwald and N. M. Johnson, J. Appl. Phys. **64**, 958 (1988).

[26] H. Zimmerman and H. Ryssel, Appl. Phys. Lett. **58**, 499 (1991).

[27] J. U. Sachse, W. Jost, and J. Weber, Appl. Phys. Lett. **71**, 1379 (1997).

[28] N. Yarykin, J. U. Sachse, H. Lemke, and J. Weber, Phys. Rev. B **59**, 5551 (1999).

[29] S. D. Brotherton, and P. Bradley, J. Appl. Phys. **53**, 5720 (1982).

[30] J. R. Troxell, PhD. thesis, Lehigh University, 1979 (unpublished).

[31] J. Wulff Petersen, O. H. Nielsen, G. Weyer, E. Antoncik, and S. Damgaard, Phys. Rev. B **21**, 4292 (1980).
[32] C. Ridder, M. Fanciulli, A. Nylandsted Larsen, and G. Weyer (unpublished).
[33] G. Weyer, S. Damgaard, J. W. Petersen, and J. Heinemeier, Hyperfine Interact. **7**, 449 (1980).
[34] G. Weyer, J. Wulff Petersen, and S. Damgaard, Hyperfine Interact. **10**, 775 (1981).
[35] Z. N. Liang, L. Niesen, G. N. van den Hoven, and J. S. Custer, Phys. Rev. B **49**, 16 331 (1994).
[36] E. M. Scherer, J. P. de Souza, C. M. Hasenack, and I. J. R. Baumvol, Semicond. Sci. Technol. **1**, 241 (1986).
[37] S. Damgaard, J. Wulff Petersen, and G. Weyer, Hyperfine Interact. **10**, 751 (1981).
[38] G. D. Watkins, Inst. Phys. Conf. Ser. **23**, 1 (1974).
[39] M. Deicher, G. Grübel, E. Recknagel, H. Skudlik, and Th. Wichert, Hyperfine Interact. **35**, 719 (1987).
[40] G. Weyer, M. Fanciulli, K. Freitag, A. Nylandsted Larsen, M. Lindroos, E. Müller, H. C. Vestergaard, and the ISOLDE Collaboration, Mater. Sci. Forum **196–201**, 1117 (1995).
[41] R. Jones and P. R. Briddon, in *Identification of Defects in Semiconductors, Vol. 51A of Semiconductors and Semimetals*, edited by M. Stavola (Academic, Boston, 1998), Chap. 6.
[42] A. Resende, R. Jones, S. Öberg, and P. R. Briddon, Phys. Rev. Lett. **82**, 2111 (1999).
[43] H. Zimmermann and H. Ryssel, Appl. Phys. Lett. **58**, 499 (1991).
[44] L. W. Song, X. D. Zhan, B. W. Benson, and G. D. Watkins, Phys. Rev. B **42**, 5765 (1990).
[45] E. Ö. Sveinbjörnsson and O. Engström, Appl. Phys. Lett. **61**, 2323 (1992).
[46] E. O. Sveinbjörnsson, G. I. Andersson, and O. Engstrom, Phys. Rev. B **49**, 7801 (1994).
[47] J. U. Sachse, J. Weber, and E. Ö. Sveinbjörnsson, Phys. Rev. B **60**, 1474 (1999).
[48] J. C. Slater, *The Self-Consistent Field for Molecules and Solids* (McGraw-Hill, New York, 1974), Vol. IV.
[49] P. M. Williams, G. D. Watkins, S. Uftring, and Michael Stavola, Phys. Rev. Lett. **70**, 3816 (1993).